MoM scattering analysis of dihedral corner reflector: TALGAT verification

Tuan Phuong Dang
Department of Television and Control
Tomsk State University of Control Systems and Radioelectronics
Tomsk, Russia
dang.p.2213-2023@e.tusur.ru

Adnan F. Alhaj Hasan
Department of Television and Control
Tomsk State University of Control Systems and Radioelectronics
Tomsk, Russia
alkhadzh@tusur.ru

Talgat R. Gazizov
Department of Television and Control
Tomsk State University of Control Systems and Radioelectronics
Tomsk, Russia
talgat.r.gazizov@tusur.ru

***Abstract*—This paper presents the results of evaluating the effectiveness of using TALGAT system that based on the Method of Moments with pulse basis function for modelling dihedral corner reflector using the wire grid approach. TALGAT backscattering and radar cross section results are compared with those obtained experimentally and numerically using other methods published in other papers. Comparisons showed high consistency, confirming the effectiveness of using TALGAT for solving such problems, as well as for generating novel sparse wire grid scatterers in the near future.**

***Keywords*—scatterer, TALGAT, method of moments, wire grid, dihedral corner reflector.**

I. Introduction

Researchers have long been interested in studying electromagnetic scattering from various structures. The development of advanced technology paved the way to the analysis of complex scattering structures. These structures are used in many fields today, including civilian [1] and military [2] applications. One of such structures that have received a significant attention are the corner reflectors [3, 4]. They have many advantages, including: high backscattering cross section (BSCS) over a wide angular range; operation without electrical power; mechanical simplicity in design; and ability to operate in harsh environments [5]. They are used in synthetic aperture radars [6], for ground target camouflage [7], and for target calibration in radar technology [8]. They also have many different shapes depending on the number of their scattering surfaces: dihedral, trihedral and octahedral etc. [9]. In this paper the dihedral corner reflector (DCR) that consists of two flat plates is considered.

In recent years, several studies focused on the analysis of perfectly conducting DCR [10, 11]. To analyze this structure, physical (PO) and geometrical (GO) optics individually or combined (PO_GO), and physical theory of diffraction (PTD) are mainly used. The effectiveness of using these methods was demonstrated by good agreement with the experimental results [12]. The special feature of these methods when analyzing corner reflectors is the necessity to take into account the number of incident wave reflections from the reflector surfaces. This number depends on the angle between the two DCR surfaces. When the DCR angle is greater than 90° only singly and doubly reflected rays contribute to the scattered field. When this angle is between 60° and 90° only singly, doubly, and triply reflected rays contribute to the scattered field. While for angles less than 60°, it is necessary to consider rays undergoing more than three reflections [13]. This increases the complexity of analyzing DCR structures.

The method of moments (MoM) is widely used in modeling various electromagnetic scattering structures such as arbitrarily shaped ones [14], wire grid (WG) [15], etc. The core process of MoM is based on converting the electric field integral equations that describe the structure under study, its boundary conditions and the excitation of it into a system of linear equations. Then through the inversion of the impedance matrix solve this system using a computer [16]. This results in the current distribution over the surface of the considered structure, which makes it possible to determine the radiated or scattered field from it. This method allows one to analyze DCR without taking into account the number of wave reflections. Due to its nature, MoM considers the mutual influence between the structure elements in its impedance matrix, while the incident wave is considered as the excitation source of these elements. MoM is a method with simple algorithm and requires less resources than other methods. It can be used with different basis functions, one of which is the pulse basis functions, that have proved their effectiveness in analyzing complex WG scattering structures [17].

TALGAT is one of the currently known MoM-based systems that can be used to solve electromagnetic problems [18]. Recently, a MoM-based scattering module with pulse basis functions has been integrated into it to analyze various WG structures. The results obtained by this module were verified for simple wire structures. However, the effectiveness of using this module needs to be evaluated by verifying its results for different structures. Moreover, it is planned to be used for generating new sparse WG scatterers by employing the recently developed optimal current grid approximation approach [19]. This increases the relevance of evaluating its performance in analyzing various WG scatterers, of which DCRs are considered to be important ones. Therefore, the aim of this paper is to verify the results of modeling DCR scatterers as WGs obtained using TALGAT system. These results are compared with those obtained numerically using PTD [20], PO_GO [21], PO [22], MoM with piecewise-sinusoidal (PWS) basis functions [23] and experimentally [20, 22, 23].

This paper is organized as follows: Section II provides the parameters of the incident plane waves, the considered DCR scatterers, and their equivalent WGs. Section III presents the BSCS and the radar cross section (RCS) reduction results of the considered scatterers using TALGAT and compares them with those published elsewhere to

This research was funded by the Ministry of Science and Higher Education of the Russian Federation project FEWM-2023-0014.

evaluate their accuracy. Section IV summarizes the study conclusions and identifies directions for future research.

II. Structures Under Study

To verify the results of MoM-based TALGAT with pulse basis functions obtained for DCR scatterers, structures of different sizes are considered. The isometric view of a solid perfectly conducting DCR structure is shown in Fig. 1*a*, while its equivalent WG structure is illustrated in Fig. 1*b*. DCR structure is formed by two rectangular plates (A and B) whose intersection coincides with the Oz axis. Both plates have a length of h, widths of w_1 and w_2 respectively. They are also symmetric with respect to the xOz plane and the angle between them is 2γ. When modeling the considered DCR structures by WG, their plates are divided into cells of equal size and edge length of Δ (Fig. 1*b*) (each WG cell edge is considered to be as one wire represented by one segment with a length equal to Δ). The value of Δ is determined as: $\lambda/6 \geq \Delta \geq \lambda/20$ [1], while the wire radius a is obtained by: $a=\Delta/2\pi$. To excite the scatterers, incident plane waves are used with linear vertical polarization (θ-polarization) and directions determined by φ^{inc} and θ^{inc}. The scattered waves have directions defined by φ^{s} and θ^{s}, and are taken as $\varphi^{s}=\varphi^{inc}$ and $\theta^{s}=\theta^{inc}$ when calculating BSCS. In this paper, we considered 6 DCR structures differing in size and angle. Their parameters and the directions of the used incident plane wave to excite them are listed in Table 1. This table also reports the methods used to analyze these structures according to the papers that considered them.

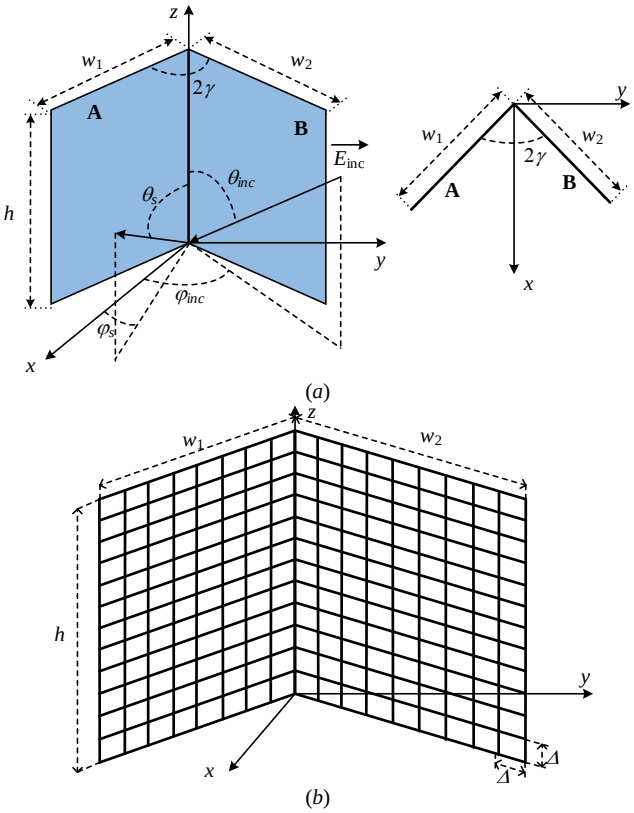

Fig. 1. DCR isometric view (*a*) and its equivalent WG (*b*).

TABLE I. Analysis Parameters of the Considered Structures

Structure	w_1, m	w_2, m	h, m	a, m	Cell numbers	φ^{inc}, °	θ^{inc}, °	f, GHz	2γ, °	Analysis
S_1 [20]	0.18	0.18	0.18	0.0009	33×33×33	0–360	90	9.4	90 98 77	PTD / measurement
S_2 [21]	7.16	4.77	4.77	0.026	43×29×29	0–360	90	0.3	90	PO+GO
S_3 [22]	2.5	2.5	5	0.019	20×20×40	0–360	90 85	0.3	85 95	PO / measurement
S_4 [22]	5	5	10	0.027	30×30×60	0–360	90	0.3	90 60	PO
S_5 [22]	6	6	10	0.024	40×40×66	0–360	90	0.3	97	PO / measured
S_6 [23]	0.5	0.5	1	0.008	10×10×20	0–360 0	90 0–360	0.3	130	MoM-PWS / measurement

III. Results

First, BSCS for S_1 with different 2γ angles are considered. Their values obtained in TALGAT are compared with those obtained experimentally and numerically using PTD in [20] (Fig. 2). It is demonstrated that TALGAT results are in an acceptable agreement with PTD results in the main lobe, but the difference between them increases in the side lobe, especially when 2γ=98 and 77°. These deviations are summarized in Table 2. It can be seen from Fig. 2*a* that the BSCS for DCR scatterer with 2γ=90° reach their maximum values at φ^{inc}=0°. They slightly change over the azimuth range of (–15°; 15°), but rapidly decrease beyond it. This is due to the fact that in this range most of the scattered energy returns in the opposite direction of the incident wave one.

TABLE II. BSCS Deviations from [20] for S_1

2γ, °	Deviations in φ^{s}=0°, θ^{s}=90°, dB		Maximum deviations, dB	
	PTD	measured	PTD	measured
90	1.3	0	10	9
98	0.2	4.8	8	6
77	0.8	1.1	8	3.8

In addition, BSCS values increase suddenly in the ranges of (–50°; –40°) and (40°; 50°). This can be explained by the fact that the plane wave had a direction almost perpendicular to one of the DCR plates. On the other hand, when 2γ=98° or 77°, the scattered energy returns in a direction that differs from the incident wave one in the main lobe region (Fig. 2*b* and 2*c*).

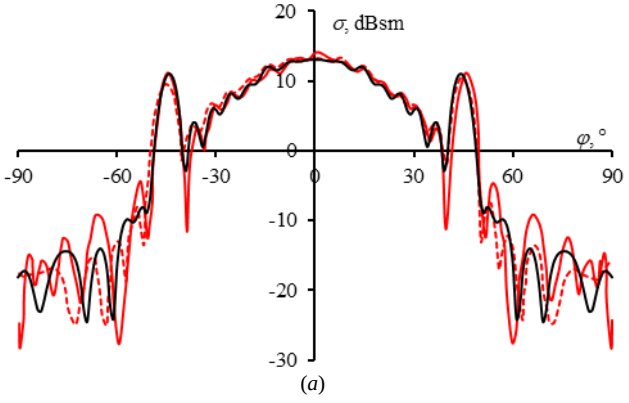

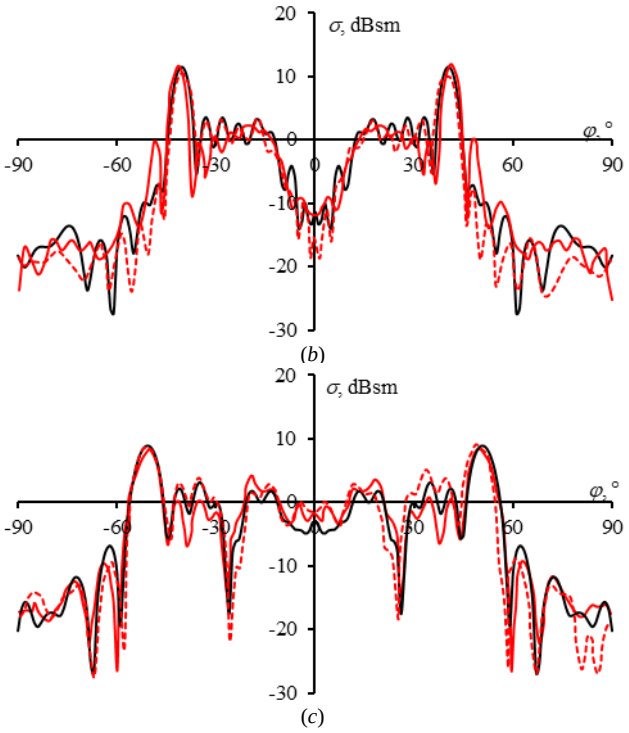

Fig. 2. BSCS for S_1 when 2γ=90° (a), 98° (b), 77° (c) obtained using TALGAT (—), PTD (—), and experimentally (----) [20].

Next, the BSCS for S_2 obtained using TALGAT were compared with those calculated using PO_GO in [21] (Fig. 3). It can be seen that TALGAT results are also in good agreement with those obtained PO_GO (their highest values differ maximumly by about 2 dB). Fig. 3 also shows that the scattered field maximums shifted by about 10° toward the side of the DCR plate with bigger width. The side lobe in the range of φ_{inc}= (40; 50) has BSCS maximum value (27.5 dB) greater than that in (–50; –40) (24.5 dB). This can be explained by the fact that plate A has a larger size than plate B, thus the scattered field from it will have a larger magnitude.

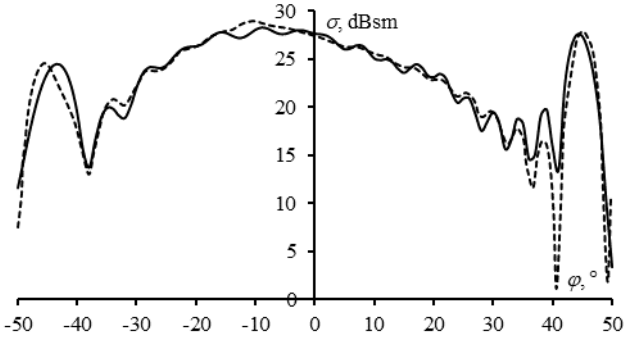

Fig. 3. BSCS for S_2 obtained using TALGAT (—) and PO_GO (----) [21].

After that, the RCS reductions for S_3 when 2γ=85° obtained using TALGAT were compared with those calculated using PO and measured in [22] (Fig. 4). These reductions are determined by the difference between the RCS values for DCRs with an angle other than 90° and their values when it is equal to it [22]. It can be seen that TALGAT results are also in good agreement with those obtained experimentally (maximum deviation is 0.8 dB). This difference is more noticeable compared to PO (maximum deviation is 1.8 dB). Nevertheless, TALGAT results agree with measurements better than PO ones.

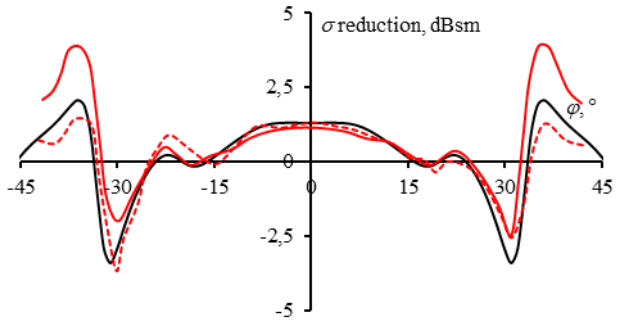

Fig. 4. RCS reductions for S_3 when 2γ=85° obtained using TALGAT (—), PO (—), and experimentally (----) [22].

Next, the BSCS for S_3 when 2γ=95° at θ^{inc}=90° and θ^{inc}=85° obtained using TALGAT were compared with those calculated using PO and measured in [22] (Fig. 5). It can be seen that TALGAT results are also in good agreement with those obtained numerically using PO (maximum deviation is less than 1.9 dB) and experimentally (maximum deviation is less than 2 dB). It can be noticed that the scattering field at θ^{inc}=90° is larger than at θ^{inc}=85°. This can be explained by the fact that at θ^{inc}=85° the maximum scattering energy will be directed to θ^{s}=95°, not in the opposite direction of the excitation wave (θ^{s}=85°).

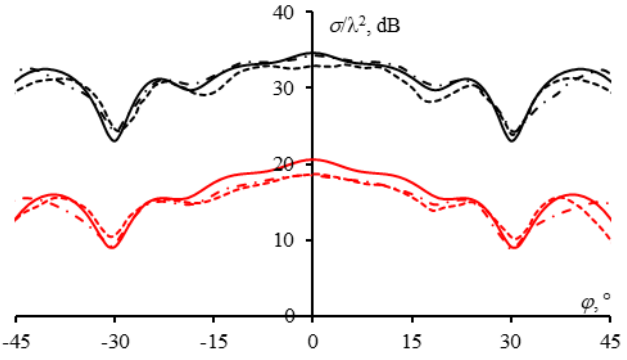

Fig. 5. BSCS for S_3 when 2γ=95° at θ_{inc}=90° (black) and θ_{inc}=85°(red) obtained using TALGAT (—), PO (–·–) and experimentally (---) [22].

Then, the calculated BSCS for S_4 when 2γ=90° and 60° using TALGAT are compared with those obtained using PO in [22] (Fig. 6). When 2γ=90°, it can be seen that TALGAT results are also in good agreement with those obtained PO (with deviation about 1 dB in φ^{inc}=0°, and maximum deviation about 3 dB). While the difference between the compared results is bigger when 2γ=60° (with deviation about 1.3 dB in φ^{inc}=0°, and maximum deviation about 13 dB).

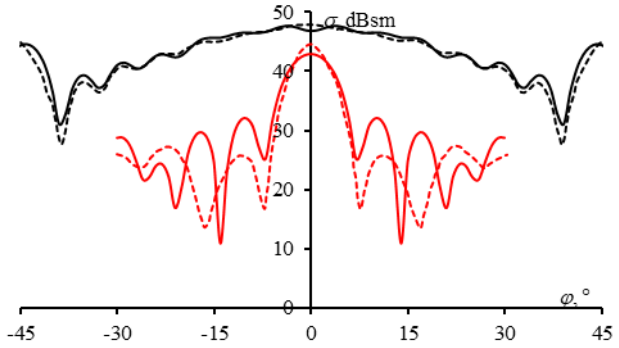

Fig. 6. BSCS for S_4 when 2γ=90°(black lines) and 2γ=60°(red lines) obtained using TALGAT (—) and PO (---) [22].

Moreover, the calculated BSCS for S_5 using TALGAT are compared with those obtained using PO and experimentally from [22] (Fig. 7). It can be seen that TALGAT results agree well with the measured results (with deviation about 1.8 dB in φ=0°, and maximum deviation about 8.6 dB). However, a larger deviation is observed by comparing them to those obtained numerically using PO (with deviation about 8.4 dB in φ=0°, and maximum deviation about 16 dB).

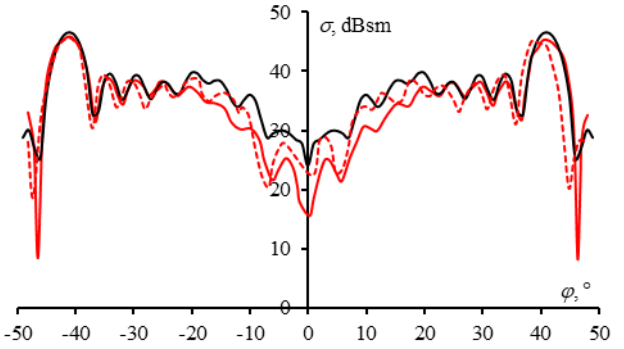

Fig. 7. BSCS for S_5 obtained using TALGAT (—), PO (—) and experimentally (---) [22].

Finally, the calculated BSCS results for S_6 in the θ=90° and φ=0° planes using TALGAT are compared with those obtained experimentally and numerically using MoM with PWS in [23] (Fig. 8). It can be seen that TALGAT results are also in good agreement with those obtained experimentally (the maximum deviation is less than 1.5 dB in the θ=90° plane and less than 0.25dB – in the φ=0° plane). Fig. 8 shows also that TALGAT results are closer to the measured ones than those of MoM with PWS. The maximum deviations calculated when comparing TALGAT and MoM with PWS results are about 9 dB in the θ=90° plane and 3.5 dB – in the φ=0° plane.

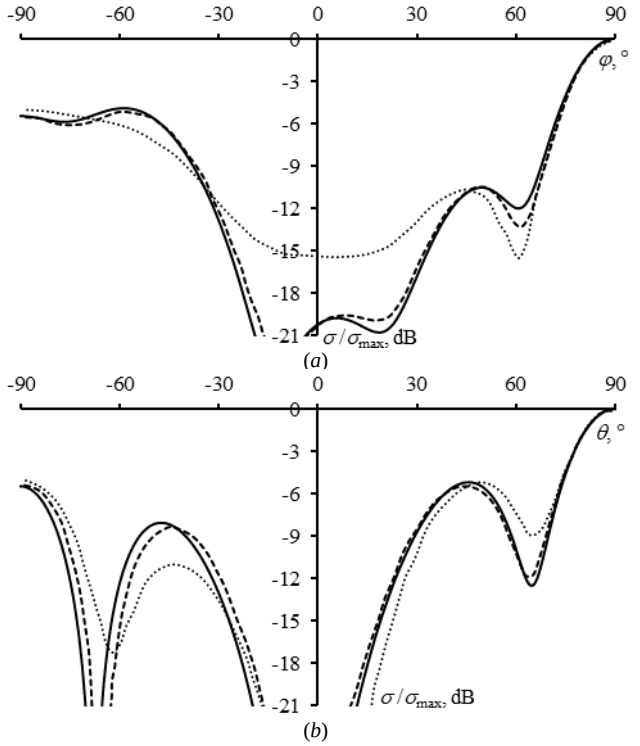

Fig. 8. BSCS for S_6 in the θ=90° (*a*) and φ=0° (*b*) planes obtained using TALGAT (—), MoM with PWS (···) and experimentally (---) [23].

In general, the results of modeling DCR scatterers using MoM-based WG with pulse basis functions in TALGAT system are quite similar to those obtained numerically using other methods and experimentally. Based on that, it evident to conclude that TALGAT can be efficiently used to analyze complex scattering structures.

IV. Conclusion

The BSCS and RCS reductions results for DCR scatterers obtained in TALGAT are verified by detailed comparisons with those obtained numerically using PTD, PO, PO_GO and experimentally in other works. These comparisons yielded a high degree of consistency, proving the accuracy and effectiveness of MoM-based TALGAT with pulse basis functions in solving such problems. This study paves the way to explore the potential of TALGAT in analyzing a wider range of complex WG scatterers. Notably, the successful verification on DCR scatterers forms the foundation for future investigations on novel sparse WG scatterers.

References

[1] M. C. Garthwaite, S. Nancarrow, A. Hislop, M. Thankappan, J.H. Dawson, and S. Lawrie, "The design of radar corner reflectors for the australian geophysical observing system: a single design suitable for InSAR deformation monitoring and SAR calibration at multiple microwave frequency bands," 2015.

[2] J. -S. Kim, D. -Y. Lee, T. -H. Kim and D. -W. Seo, "Chaff cloud modeling and electromagnetic scattering properties estimation," in IEEE Access, vol. 11, pp. 58835-58849, 2023, doi: 10.1109/ACCESS.2023.3284833.

[3] T. Jiang, J. Luo and Z. Yu, "Research on corner reflector array fitting method for ship scattering characteristics," 2023 IEEE 2nd International Conference on Electrical Engineering, Big Data and Algorithms (EEBDA), Changchun, China, 2023, pp. 1309–1313, doi: 10.1109/EEBDA56825.2023.10090547.

[4] K. Zhang, J. Zhang, C. Li, S. Li and C. Lan, "Combined jamming method of chaff and corner reflector against anti-ship missiles," 2024 IEEE 7th Advanced Information Technology, Electronic and Automation Control Conference (IAEAC), Chongqing, China, 2024, pp. 342–346, doi: 10.1109/IAEAC59436.2024.10503679.

[5] I. Hanninen, M. Pitkonen, K. I. Nikoskinen and J. Sarvas, "Method of moments analysis of the backscattering properties of a corrugated trihedral corner reflector," in IEEE Transactions on Antennas and Propagation, vol. 54, no. 4, pp. 1167–1173, April 2006, doi: 10.1109/TAP.2006.872676.

[6] Ye Xia, H. Kaufmann and Xiaofang Guo, "Differential SAR interferometry using corner reflectors," IEEE International Geoscience and Remote Sensing Symposium, Toronto, Ontario, Canada, 2002, pp. 1243-1246, vol. 2, doi: 10.1109/IGARSS.2002.1025902.

[7] J. Hao, X. Wang, S. Yang, H. Gao, C. Yu, and W. Xing, "Intelligent target design based on complex target simulation," Applied Sciences, vol. 12, pp. 8010, 2022.

[8] F. Gibert et al., "A trihedral corner reflector for radar altimeter calibration," in IEEE Transactions on Geoscience and Remote Sensing, vol. 61, pp. 1–8, 2023, doi: 10.1109/TGRS.2023.3239988.

[9] C. Händel, H. Konttaniemi, and M. Autioniemi, "State-of-the-art review on automotive radars and passive radar reflectors: Arctic challenge research project," 2018.

[10] A. N. Yakimov, A. R. Bestugin and I. A. Kirshina, "Parametric optimization of the corner reflector of electromagnetic waves," 2022 Wave Electronics and its Application in Information and Telecommunication Systems (WECONF), St. Petersburg, Russian Federation, 2022, pp. 1–4.

[11] J. Gu, F. Dai, Q. Chen, D. Gu, Y. Liao and B. Wang, "Research on RCS calculation and weight loss method of radar angle reflector," 2022 3rd China International SAR Symposium (CISS), Shanghai, China, 2022, pp. 1–4, doi: 10.1109/CISS57580.2022.9971366.

[12] P. Corona, G. Ferrara and C. Gennarelli, "Backscattering by loaded and unloaded dihedral corners," in IEEE Transactions on Antennas

and Propagation, vol. 35, no. 10, pp. 1148–1153, October 1987, doi: 10.1109/TAP.1987.1143986.

[13] W. Anderson, “Consequences of nonorthogonality on the scattering properties of dihedral reflectors,” in IEEE Transactions on Antennas and Propagation, vol. 35, no. 10, pp. 1154 1159, October 1987, doi: 10.1109/TAP.1987.1143993.

[14] S. Rao, D. Wilton and A. Glisson, “Electromagnetic scattering by surfaces of arbitrary shape,” in IEEE Transactions on Antennas and Propagation, vol. 30, no. 3, pp. 409–418, May 1982, doi: 10.1109/TAP.1982.1142818.

[15] J. Richmond, “A wire-grid model for scattering by conducting bodies,” in IEEE Transactions on Antennas and Propagation, vol. 14, no. 6, pp. 782–786, November 1966, doi: 10.1109/TAP.1966.1138783.

[16] P. T. Dang, A. F. Alhaj Hasan and T. R. Gazizov, “Analyzing the wire scatterer using the method of moments with the step basis functions," XXVII International Conference 2024 Wave electronics and its application in information and telecommunication systems (WECONF), Saint-Petersburg, Russia, 2024. To be published.

[17] P. T. Dang, A. F. Alhaj Hasan and T. R. Gazizov, “Wire grid scatterer modeling: TALGAT verification," International Russian Automation Conference(RusAutoCon), Sochi, Russia, 2024. To be published.

[18] TALGAT software. Available online: https://talgat.org/talgat-software/ (accessed Apr. 20, 2024).

[19] T. Griesser and C. Balanis, “Backscatter analysis of dihedral corner reflectors using physical optics and the physical theory of diffraction,” in IEEE Transactions on Antennas and Propagation, vol. 35, no. 10, pp. 1137–1147, October 1987, doi: 10.1109/TAP.1987.1143987.

[20] A. Alhaj Hasan, T. M. Nguyen, S. P. Kuksenko and T. R. Gazizov, “Wire-grid and sparse MoM antennas: past evolution, present implementation and future possibilities,” Symmetry, 2023, vol. 15(2), p. 378. doi: 10.3390/sym15020378.

[21] E. Knott, “RCS reduction of dihedral corners,” in IEEE Transactions on Antennas and Propagation, vol. 25, no. 3, pp. 406–409, May 1977, doi: 10.1109/TAP.1977.1141586.

[22] W. Anderson, “Consequences of nonorthogonality on the scattering properties of dihedral reflectors,” in IEEE Transactions on Antennas and Propagation, vol. 35, no. 10, pp. 1154–1159, October 1987, doi: 10.1109/TAP.1987.1143993.

[23] N. N. Wang, “Reaction formulation for radiation and scattering from plates corner reflectors and dielectric coated cylinders,” The Ohio State University, 1974.